RESEARCH ARTICLE

Commutation Failure Predictive Control Based on Fast AC Voltage Measurement in LCC-HVDC

GUODONG HUANG[1], XIAO TIAN[2], HAIBO YUAN[3], XIAOFENG DONG[1], LI ZHOU[1], AND QING WANG[1]

[1]State Grid Suzhou Power Supply Company, Suzhou, Jiangsu 215004, China
[2]Faculty of Electric Power Engineering, Kunming University of Science and Technology, Kunming, Yunnan 650500, China
[3]Anhui Nari Jiyuan Electric Network Technology Company Ltd., Hefei 230088, China

Corresponding author: Xiao Tian (3130158063@qq.com)

ABSTRACT To inhibit commutation failure (CF), in this paper, the influence factors of CF were analyzed, and considering different fault types and different valves, the mathematical expression of extinction angle was deduced. In addition, by analyzing existing control strategies for inhibiting CF, it is indicated that existing control strategies cannot quickly and accurately obtain the AC voltage amplitude and zero-crossing phase shift angle. To solve this problem, this paper proposed a fast AC voltage measurement method, and the zero-crossing phase shift angle can be calculated by AC voltage amplitude. On this basis, a commutation failure predictive control method (CFPCM) was proposed to inhibit CF. The CFPCM can adapt to all fault types. Finally, based on the CIGRE HVDC benchmark model, the commutation failure prevention module (CFPREV) and CFPCM simulation model were built using PSCAD/EMTDC to verify the effectiveness of the proposed CFPCM. The simulation results showed that the CFPCM can not only inhibit CF more effectively, but also reduce the fluctuation of DC current, AC voltage, and extinction angle with a fault occurred in the inverter AC system.

INDEX TERMS Commutation failure, DC current, HVDC, predictively control, extinction angle.

I. INTRODUCTION

China has built the largest AC-DC hybrid power grid with the highest voltage level all over the world [1]. All regional power grids have been interconnected through Ultra-High Voltage Direct Current (UHVDC) transmission lines, with 23 HVDC lines taking 34% of the transmission power [2], [3]. As increasing numbers of UHVDC systems are put into operation, the coupling between AC and DC systems is becoming closer. At present, the power system is presenting strong DC and weak AC system characteristics [4], [5]. Commutation failure (CF) is the most common fault of DC systems, which can cause drastic fluctuations in current, voltage, and power [6]. Generally, most CFs are caused by faults occurred in the inverter AC system. According to the statistics, from 2004 to 2018, a total of 1 353 CFs occurred in 21 HVDC transmission systems operated by the State Grid

Corporation of China (SGCC), and among them, 1 209 CFs were caused by inverter AC system faults, accounting for 89.36%, and 144 CFs were caused by an abnormal valve control system, accounting for 10.64% [7]. When a fault occurred in the inverter AC system, it may lead to the CF, causing a serious impact on the safe and stable operation of the power grids.

To prevent the CF, many scholars focus on the CF mechanism and the improvement DC control strategy. The low extinction angle is the fundamental reason for CF. A decrease of inverter AC system voltage and an increase DC current will affect the extinction angle [8]. To inhibit CF, various inverter firing angle control strategies were proposed, such as an extinction angle detection method and a constant extinction angle control strategy were proposed in [9] and [10], an AC system fault voltage detection method was also proposed [11]. Based on this, a commutation failure prevention method (CFPREV) was proposed in [12], which have been widely used in practical projects and can realize fast detecting

inverter AC voltage to inhibit CF. However, only symmetrical and asymmetric faults can be identified by CFPREV, and the AC voltage amplitude cannot be obtained quickly, hence, the advance firing angle given by CFPREV may not be accurate, leading to the reactive power consumed by inverter to increase.

In addition, a fuzzy controller was proposed in [13] and [14]. Considering the inverter AC voltage distortion, Liu et al. [15] proposed an extinction angle predictive control strategy. Qi et al. [16] proposed a CF predictive method that considers the effect of DC current variation on the extinction angle. An algorithm was proposed to predict DC current and limit the effect of DC current on CF [17], [18]. However, the proposed control method faces the same problem as CFPREV.

To control the extinction angle more accurately and avoid the reactive power consumption caused by advance firing angle, Mirsaeidi et al. [19] considered the DC current variation and equivalent inductance, proposed a commutation failure inhibition module (CFIM), which can accurately predict the overlap area and inhibit CF. Further, considering different inverter AC system fault types, a commutation failure prevention module (CFPM) was also proposed in [20]. However, the CFIM needs a time detector to measure the trigger pulse time and the overlap angel time, and the CFIM is complex and requires the high precision measuring elements and it is related to a PMU and needs to reform greatly, as it is uneconomical from the cost viewpoint. Based on the virtual resistance, a variable extinction angle control strategy is proposed to inhibit CF [21]. Considering the influence of initiation time on the extinction angle, a novel prediction and prevention for inhibit CF is proposed in [22]. For the multi-infeed HVDC system, the mechanism of anomalous CF was analyzed, and the inhibition strategy was proposed in [23]. However, the problem of above methods is same as CFPREV. In addition, in [24], the influence of harmonic components on the CF was analyzed, and a predictive CF inhibition control strategy was proposed. In [25] and [26], from the perspective of converter topology transformation, multi-type converter topologies were proposed, which can inhibit CF more effective. However, there are problems of too long reformation time and poor economy, and there is no practical application.

Thyristor as the main device of LCC-HVDC, a thyristor has the characteristics of one-way controllability, i.e., its turn-on can be controlled, but not its turn-off. When the voltage on the thyristor valve is positive, a firing pulse is given to the thyristor valve, the valve will turn on. To turn-off a thyristor valve, it is necessary to apply a reverse voltage to the valve, which is highly dependent on AC voltage. Hence, CF as inherent defect of thyristor, it cannot be fully suppressed. Moreover, when a fault occurred in the inverter AC system, the CF will occur quickly (within a few ms), due to the smooth reactor configured in the both ends of HVDC system, the DC current will not change significantly during the time of fault to CF. Most control strategies are relied on the AC voltage
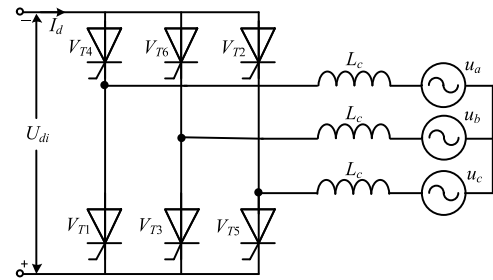

FIGURE 1. Graetz bridge.

amplitude, the fast AC voltage amplitude measurement is the most important for inhibiting first CF. However, the existing control strategy adopted the traditional measurement methods, it will cost at least 10 ms to accurate measurement of AC voltage amplitude, which cannot meet the requirements of CF. In addition, although the CFPREV can detect the AC fault quickly, however, the voltage amplitude for the asymmetric fault cannot obtained.

To handle above problem, in this paper, a fast AC voltage measurement method is proposed, the AC voltage amplitude can be obtained quickly and accurately for all fault types, based on this, a commutation failure predictive control module (CFPCM) was proposed instead of CFPREV, the CFPCM is easy to realize and it can control extinction angle accurately.

The remainder of this paper is organized as follows: In Section II, the CF mechanisms with different fault types are analyzed. In Section III, existing control strategies and problems to inhibit CF are introduced. Section IV provides the function of fast AC voltage measurement method and proposed CFPCM to inhibit CF. The CFPCM and CFPREV simulations were carried out using PSCAD/EMTDC presented in Section V. Finally, the conclusions are given in Section VI.

II. COMMUTATION FAILURE AND AC FAULT
The most commonly used converter unit, the structure of 6-pulse inverter (also called Graetz bridge) is shown in Fig. 1 [19], comprising six thyristor valves (V_{T1}, V_{T2}, V_{T3}, V_{T4}, V_{T5}, and V_{T6}). In Fig. 1, the L_c is the equivalent commutation inductance; u_a, u_b, and u_c are the instantaneous values of commutation voltage; U_{di} is the DC voltage of the inverter; I_d is the DC current of the inverter.

A thyristor has the characteristics of one-way controllability, i.e., its turn-on can be controlled, but not its turn-off. When the voltage on the thyristor valve is positive, a firing pulse is given to the thyristor valve, the valve will turn on, and the corresponding firing pulse is referred to as firing angle of the inverter (α_i). Owing to the L_c, the commutation from one valve to another valve cannot complete instantaneously and requires a certain time, referred to as overlap angle (μ). To turn-off a thyristor valve, it is necessary to apply a reverse voltage to the valve. Once the normal commutation of the two commutation valves is completed, the thyristor valves need
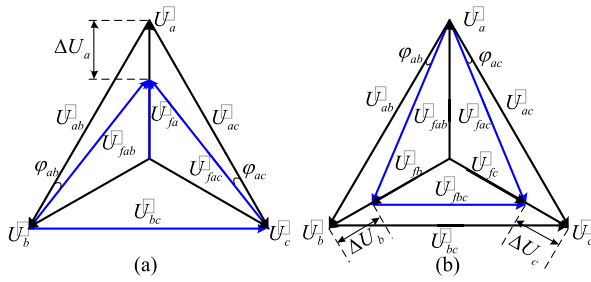
FIGURE 2. The phasor diagram under LG and LLG faults; (a) the phase-a to ground fault; (b) the phase-b and phase-c to ground fault.

to withstand reverse voltage for a certain time to restore their blocking capacity, and this time is referred to as extinction angle (γ). According to Fig. 1, the extinction angle of each valve can be expressed as [27]

$$\begin{cases} \gamma_{V_{T1},V_{T4}} = \arccos(\dfrac{\sqrt{2}\,X_{ci}I_d}{T_iU_{ab}} + \cos\beta_{V_{T1},V_{T4}}) - \varphi_{ab} \\ \gamma_{V_{T2},V_{T5}} = \arccos(\dfrac{\sqrt{2}\,X_{ci}I_d}{T_iU_{ac}} + \cos\beta_{V_{T2},V_{T5}}) - \varphi_{ac} \\ \gamma_{V_{T3},V_{T6}} = \arccos(\dfrac{\sqrt{2}\,X_{ci}I_d}{T_iU_{bc}} + \cos\beta_{V_{T3},V_{T6}}) - \varphi_{bc} \end{cases} \quad (1)$$

where X_{ci} is the commutation reactance of inverter ($X_{ci} = \omega L_c$); β is the advanced firing angle of the inverter; the line-line voltage U_{ab}, U_{bc}, and U_{ac} are the RMS values between phases a, b, and c. The φ_{ab}, φ_{ac} and φ_{bc} are the zero-crossing phase shift angle of line to line voltage (U_{ab}, U_{ac} and U_{bc}) respectively.

Since the three-phase voltages are $2/3\pi$ out of phase with each other, the u_a, u_b, and u_c can be expressed as

$$\begin{cases} u_a = \sqrt{2}\,U_a\cos(\omega t) \\ u_b = \sqrt{2}\,U_b\cos(\omega t + \dfrac{2}{3}\pi) \\ u_c = \sqrt{2}\,U_c\cos(\omega t - \dfrac{2}{3}\pi) \end{cases} \quad (2)$$

where U_a, U_b, and U_c are the effective value of phase a, b, and c. The ω is the angular frequency.

The common types of faults taking place on a transmission line are listed as following: (1) three-phase to ground fault (LLLG) fault; (2) double line to ground (LLG) fault; (3) single-line to ground (LG) fault. For the LLG and LG faults, the phasor diagram can be shown in Fig. 2.

In Fig. 2, the ΔU_a, ΔU_b, and ΔU_c are the voltage drops of phase a, b, and c, respectively. The subscript f indicates the voltage caused by a fault.

As shown in Fig. 2(a), when an LG fault occurred in the inverter AC system, assuming the U_b and U_c remain unchanged, the U_{ac} and U_{bc} will decrease, and U_{bc} remains unchanged. Moreover, the φ_{ac} and φ_{ab} will increase, according to (1), the $\gamma_{V_{T1}}$, $\gamma_{V_{T4}}$ and $\gamma_{V_{T2}}$, $\gamma_{V_{T5}}$ will decrease, and this will eventually increase the CF risk in the V_{T1}, V_{T4}, V_{T2}, and V_{T5}. For the LLG fault, the U_{ac}, U_{bc}, and U_{ab} will all

decrease, and the φ_{ab} and φ_{ac} will increase, the φ_{bc} is still 0, according to (1), all valves may face CF. For the LLLG fault, as the voltage has the same amplitude, it can be considered that the φ_{ab}, φ_{ac}, and φ_{bc} are all 0. Therefore, For an LLG fault, the effect of LLG fault on CF can be equivalent to the superposition of LG and LLG faults.

Therefore, the reason and mechanism of CF for different fault types in the inverter AC system are also different, to inhibit CF accurately, the control strategies should be different as well.

III. EXISTING INVERTER CONTROL STRATEGIES
For an LCC-HVDC, the control strategies play a very significant role to ensure the stability and security of the HVDC transmission. The strategy in the inverter control system determines the ability of DC systems to resist commutation failure. At present, there are two main control strategies in HVDC projects, which are ABB strategies, and SIEMENS strategies. For the ABB control strategies, a predictive control is adopted, and this can be expressed as [19].

$$\beta = \arccos(-\cos\gamma_{ref} + \frac{\sqrt{2}\,X_{Ci}I_d}{U_{Li}} + k(I_{dref} - I_d)) \quad (3)$$

where γ_{ref} is the extinction angle order value; I_{dref} is the DC current order value, which is from voltage dependent current order limiter (VDCOL), U_{Li} is the line to line RMS voltage of inverter converter bus, it can be taken place by U_{ab}, U_{ac}, and U_{bc} in (1), respectively, $k(I_{dref}\text{-}I_d)$ is a correction term, where k is the proportion factor and is required to be greater than 0.

For the SIEMENS control strategy, when a fault occurs at the inverter side, the γ drops rapidly, the $\Delta\gamma$ increases, and the CEA control will reduce the α_i to prevent CF. Although it can control extinction angle accurately, it is too slow to prevent CF due to the PI controller.

According to (3), in order to obtain the U_{Li}, it will take at least half cycle time (For 50 HZ system, it is 0.01 s). Moreover, when a fault occurs at the inverter side, the I_d increases, and the VDCOL tends to decrease I_{dref} for the decreasing of U_{di}. The $k(I_{dref} - I_d) < 0$, according to (3), will make β smaller that increases the risk of the CF. Therefore, it will lead to the CF, which cannot be inhibited in the initial stage of the fault. To overcome this problem, the commutation failure prevention (CFPREV) module is proposed to advance the firing angle. The CFPREV can detect the AC system voltage drops quickly and compensate the effect of φ, hence, it can well make up for the deficiency of (3). The AC system voltage detection module in CFPREV can be expressed as [12].

$$\begin{bmatrix} V_\alpha \\ V_\beta \end{bmatrix} = \begin{bmatrix} \frac{2}{3} & -\frac{1}{3} & -\frac{1}{3} \\ 0 & \frac{\sqrt{3}}{3} & -\frac{\sqrt{3}}{3} \end{bmatrix} \begin{bmatrix} u_a \\ u_b \\ u_c \end{bmatrix} \quad (4)$$

$$V_{\alpha\beta} = \sqrt{V_\alpha^2 + V_\beta^2} \quad (5)$$

$$|3U_0| = |u_a + u_b + u_c| \quad (6)$$

According to (5) and (6), the phasor diagram can be shown as Fig. 3.
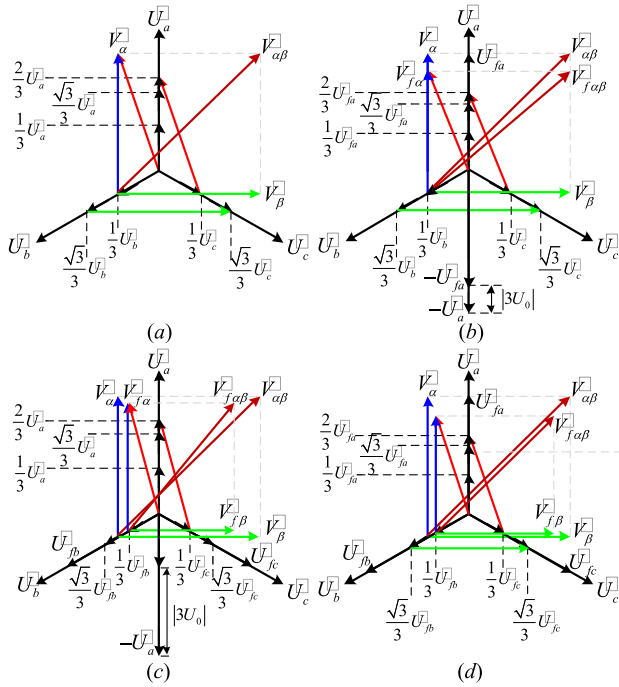
FIGURE 3. The *abc/α β* phasor diagram under different fault types; (a) the normal condition; (b) LG fault; (c) LLG fault; (d) LLLG fault.

In Fig. 3, the U_{fa}, U_{fb} and U_{fc} are the voltage amplitude with fault of phase a, b and c, respectively. The U_{fab}, U_{fac} and U_{fab} are the line to line voltage effective value with fault.

As shown in Fig. 3(a), in the normal operation model, the three phase voltage has the same amplitude, the $|V_\alpha| = |V_\beta|$, $\dot{V}_\alpha$ leads $\dot{V}_\beta$ $\pi/2$, and according to (5), the $V_{\alpha\beta}$is a scalar quantity, $V_{\alpha\beta} = \sqrt{2} \, U_a = (\sqrt{2}/\sqrt{3})U_{Li}$. When an LLLG fault occurs at the inverter AC system, as shown in Fig. 3(d), the three-phase voltage remains with the same amplitude, therefore, $V_{\alpha\beta}$ indicates the voltage amplitude drops with an LLLG fault. When an LG fault or LLG fault occurs at the inverter AC system, as shown in Figs. 3(b) and (c), the $|V_{f\alpha}| \neq |V_{f\beta}|$, hence, the $V_{f\alpha\beta}$ will be a vector, and it cannot express the voltage amplitude after an LG fault. According to (6), the $|3U_0|$ will be not 0, but $|3U_0|$is the vector that the same direction as phase-a. Therefore, the $abc/\alpha\beta$ can detect the symmetric and asymmetric faults quickly, but it cannot obtain fault types and voltage amplitude after fault except LLLG fault. Moreover, the $abc/\alpha\beta$ does not reflect the φ. Hence, the commutation failure predictive method, which adopted the $abc/\alpha\beta$ cannot control the firing angle of inverter accurately, when the firing angle is not enough, it may lead to the CF, when the firing angle is too large, it may lead to the reactive power consumed by inverter increases, further decreasing the AC voltage, which in turn increase the CF risk.

IV. PROPOSED CONTROL STRATEGY
A. EXTINCTION ANGLE MATHEMATICAL MODEL
According to (2), in the normal operation model, the three-phase voltage has the same amplitude, then the line-to-line voltage zero-cross point can be calculated as $\pi/6$.
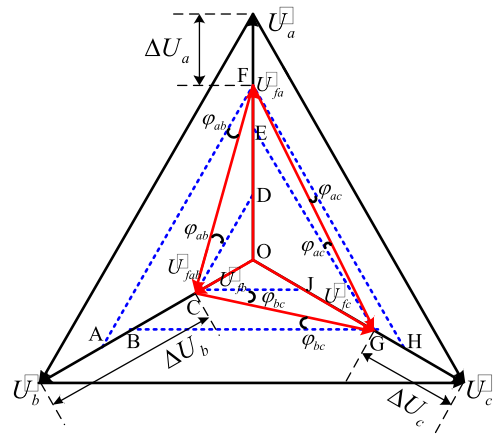
FIGURE 4. The voltage phasor diagram with any fault type.

For any fault types, the voltage phasor diagram is shown in Fig. 4. To express the relationship between various quantities conveniently, key nodes are represented by $A\sim J$.

As shown in Figure 4, the $\Delta U_a \neq \Delta U_b \neq \Delta U_c$, assuming the phase voltage $U_p = U_a = U_b = U_c$ in normal operation model, according to Fig. 4, the φ_{ab}, φ_{ac}, and φ_{bc} can be calculated by (7).

$$\begin{cases} \varphi_{ab} = \arccos(\dfrac{AF^2 + CF^2 - AC^2}{2AF \times CF}) \\ \varphi_{ac} = \arccos(\dfrac{FH^2 + FG^2 - GH^2}{2FH \times FG}) \\ \varphi_{bc} = \arccos(\dfrac{BG^2 + CG^2 - BC^2}{2CG \times BG}) \end{cases} \quad (7)$$

where $AF = FH = \sqrt{3} \, U_{fa}$, $BG = \sqrt{3} \, U_{fb}$, $AC = U_{fa} - U_{fb}$, $GH = U_{fa} - U_{fc}$and $BC = U_{fc} - U_{fb}$. The CF, FG, and CGcan be expressed as

$$\begin{cases} CF = \sqrt{U_{fa}^2 + U_{fb}^2 + U_{fa}U_{fb}} \\ FG = \sqrt{U_{fa}^2 + U_{fc}^2 + U_{fa}U_{fc}} \\ CG = \sqrt{U_{fb}^2 + U_{fc}^2 + U_{fb}U_{fc}} \end{cases} \quad (8)$$

Then, Eq. (7) can be expressed as

$$\begin{cases} \varphi_{ab} = \arccos(\dfrac{\sqrt{3}(U_{fa} + U_{fb})}{2\sqrt{U_{fa}^2 + U_{fb}^2 + U_{fa}U_{fb}}}) \\ \varphi_{ac} = \arccos(\dfrac{\sqrt{3}(U_{fa} + U_{fc})}{2\sqrt{U_{fa}^2 + U_{fc}^2 + U_{fa}U_{fc}}}) \\ \varphi_{bc} = \arccos(\dfrac{\sqrt{3}(U_{fb} + U_{fc})}{2\sqrt{U_{fb}^2 + U_{fc}^2 + U_{fb}U_{fc}}}) \end{cases} \quad (9)$$

According to Fig. 4 and (8), the $U_{fab} = CF$, $U_{fac} = FG$, and $U_{fbc} = CG$. Then, according to (1), the γ can be
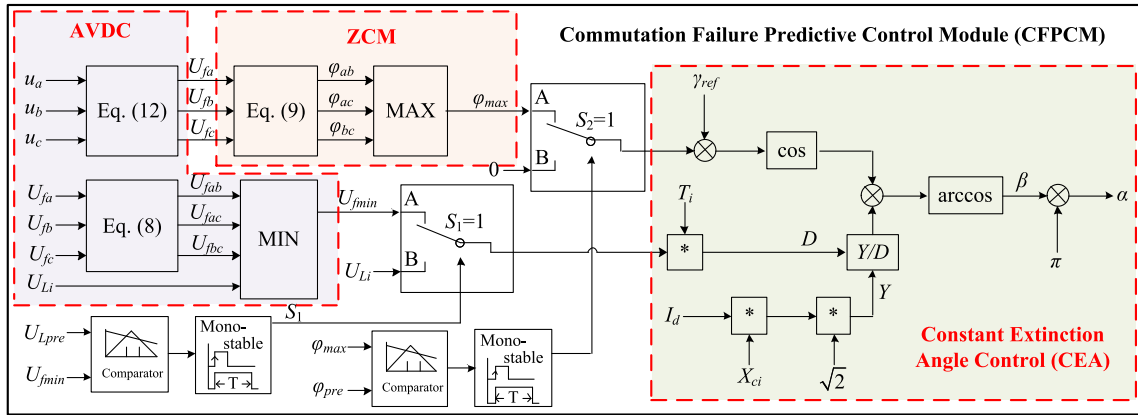
FIGURE 5. Schematic diagram of the proposed commutation failure predictive control.

calculated as

$$
\begin{cases}
\gamma_{V_{T1},V_{T4}} = \arccos\left(\dfrac{\sqrt{2}\,X_{ci}I_d}{T_i\sqrt{U_{fa}^2 + U_{fb}^2 + U_{fa}U_{fb}}} + \cos\beta_{V_{T1},V_{T4}}\right) \\
\qquad - \arccos\left(\dfrac{\sqrt{3}(U_{fa}+U_{fb})}{2\sqrt{U_{fa}^2 + U_{fb}^2 + U_{fa}U_{fb}}}\right) \\
\gamma_{V_{T2},V_{T5}} = \arccos\left(\dfrac{\sqrt{2}\,X_{ci}I_d}{T_i\sqrt{U_{fa}^2 + U_{fc}^2 + U_{fa}U_{fc}}} + \cos\beta_{V_{T2},V_{T5}}\right) \\
\qquad - \arccos\left(\dfrac{\sqrt{3}(U_{fa}+U_{fc})}{2\sqrt{U_{fa}^2 + U_{fc}^2 + U_{fa}U_{fc}}}\right) \\
\gamma_{V_{T3},V_{T6}} = \arccos\left(\dfrac{\sqrt{2}\,X_{ci}I_d}{T_i\sqrt{U_{fb}^2 + U_{fc}^2 + U_{fb}U_{fc}}} + \cos\beta_{V_{T3},V_{T6}}\right) \\
\qquad - \arccos\left(\dfrac{\sqrt{3}(U_{fb}+U_{fc})}{2\sqrt{U_{fb}^2 + U_{fc}^2 + U_{fb}U_{fc}}}\right)
\end{cases}
$$

$$(10)$$

According to (10), the extinction angle is related to the voltage amplitude of every phase, when the U_{fa}, U_{fb}, and U_{fc} can be detected quickly, the extinction angle can be under any fault types can be calculated by (10). When an LLLG fault occurs at the inverter AC system, the $U_{fa} = U_{fb} = U_{fc}$, then according to (9), the φ can be calculated as 0, hence, (10) can be adapted to all the fault types.

B. COMMUTATION FAILURE PREDICTIVE CONTROL

To get the voltage amplitude quickly, according to (2), du_a/dt, du_b/t, and du_c/dt can be expressed as

$$
\begin{cases}
\dfrac{du_a}{dt} = -\sqrt{2}\,\omega U_a \sin(\omega t) \\
\dfrac{du_b}{dt} = -\sqrt{2}\,\omega U_b \sin\left(\omega t + \dfrac{2}{3}\pi\right) \\
\dfrac{du_c}{dt} = -\sqrt{2}\,\omega U_c \sin\left(\omega t - \dfrac{2}{3}\pi\right)
\end{cases}
$$

$$(11)$$

According to (1) and (11), $du_a/\omega dt$ has the same amplitude ass u_a, and they are out of phase by $\pi/2$. For u_b and u_c, it is

the same as u_a. Hence, according to Fig. 4, even if the $\Delta U_a \neq \Delta U_b \neq \Delta U_c$, the voltage amplitude can be calculated by (12).

$$
\begin{cases}
U_{fa} = \sqrt{\left(u_a^2 + \left(\dfrac{du_a}{\omega dt}\right)^2\right)/2} \\
U_{fb} = \sqrt{\left(u_b^2 + \left(\dfrac{du_b}{\omega dt}\right)^2\right)/2} \\
U_{fc} = \sqrt{\left(u_c^2 + \left(\dfrac{du_c}{\omega dt}\right)^2\right)/2}
\end{cases}
$$

$$(12)$$

The U_{fa}, U_{fb}, and U_{fc} with any fault types can be obtained quickly and precisely by (12).

According to (10) and (12), a novel CFPCM is shown in Fig. 5.

As shown in Fig. 5, the CFPCM consists of AC voltage detection and calculation module (AVDC), according to (10) and (12), the voltage amplitude after fault (line-to-line voltage and phase voltage amplitude) can be calculated fast by AVDC. The ZCM is the zero-crossing phase shift angle module, and based on (9), the φ_{ab}, φ_{ac}, and φ_{bc} can be obtained. In addition, the CEA control is adopted by (10), when the γ is γ_{ref}, the β can be calculated. Moreover, the $U_{Li,pre}$ and φ_{pre} in Fig.5 are the pre-set value of line-to-line RMS voltage and zero-crossing angle phase shift angle, respectively, the $U_{f\min}$ and $\varphi_{\max}$ can be expressed as

$$
\begin{cases}
U_{f\min} = \min(U_{fab}, U_{fac}, U_{fbc}) \\
\varphi_{\max} = \max(\varphi_{ab}, \varphi_{bc}, \varphi_{ac})
\end{cases}
$$

$$(13)$$

When the $U_{f\min}$ detected and calculated by AVDC is smaller than $U_{Li,pre}$, it will make the $S_1 = 1$, and it will choose the $U_{f\min}$ as the line-to-line RMS voltage for CEA, similarly, when the $\varphi_{\max}$ is greater than φ_{pre}, it will drive the CEA to choose the $\varphi_{\max}$.

V. CASE STUDY

Based on CIGRE HVDC Benchmark model [28] and ABB control strategies, the simulation model with CFPREV and CFPCM were built in the PSCAD/EMTDC to validate the
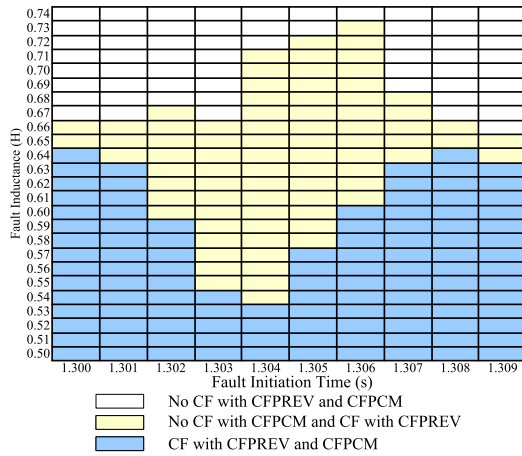
FIGURE 6. Simulation results for the LG fault with different fault inductances and fault initiation times.

FIGURE 7. Simulation results for the LLG fault with different fault inductances and fault initiation times.

FIGURE 8. Simulation results for LLLG fault with different fault inductances and fault initiation time.

effectiveness of the proposed CFPCM in this paper. The simulation model structure can be shown in APPENDIX A, Fig. 14, the detail model parameters can be seen in [29]. The pulse duration for the monostable is set as 0.05 s in Fig. 5, and the $U_{Li,pre}$ and φ_{pre} is set as 0.85 and 0.1, respectively.

In this paper, with different fault inductances (L_f) and fault initiation times (1.300s to 1.3009s), LG fault (L_f varies from 0.50 H to 0.74 H), LLG fault (L_f varies from 0.85 H to 1.19 H)), and LLG fault (L_f varies from 0.90 H to 1.32 H) were applied at the inverter AC converter bus, and all the fault duration was set as 0.1 s. The simulation results of the CF for LG fault, LLG fault, and LLG fault with different fault inductances and fault initiations are shown in Fig. 6, 7, and 8, respectively.

As shown in Fig. 6, the proposed control strategy (CFPCM) can prevent CF more effectively for all fault initiation times. When the fault initiation time is 1.304 s, CFPREV can only prevent 0.72 H of L_f from CF, however, by applying CFPCM, the inverter can inhibit CF when L_f is 0.54 H.

Fig. 7 shows the simulation results of the CF for an LLG fault with different fault inductances and initiation times, compared to CFPREV, the CFPCM can inhibit CF more effectively, especially at 1.302 s, the CFPCM can prevent 0.86 H of L_f from CF.

The simulation results from Fig. 8 indicate that the CFPCM greatly reduced the critical fault inductance of inverter commutation failure. By applying CFPREV, the most critical fault inductance is 1.30 H, after applying CFPCM, the critical fault inductance is approximately 0.96 H at all fault initiation times.

Fig. 9 shows the simulation results of the system performance in an LG fault at 1.304s and its duration is 0.1s when the L_f is 0.6 H and 0.8 H, respectively. Fig. 9(a) clearly shows no CF by applying CFPCM, but it occurs by applying CFPREV at an L_f of 0.6H. The γ, by applying CFPREV, decreases to 0 for some time, but by applying CFCCS proposed in this study, the extinction angle (γ) remains at a
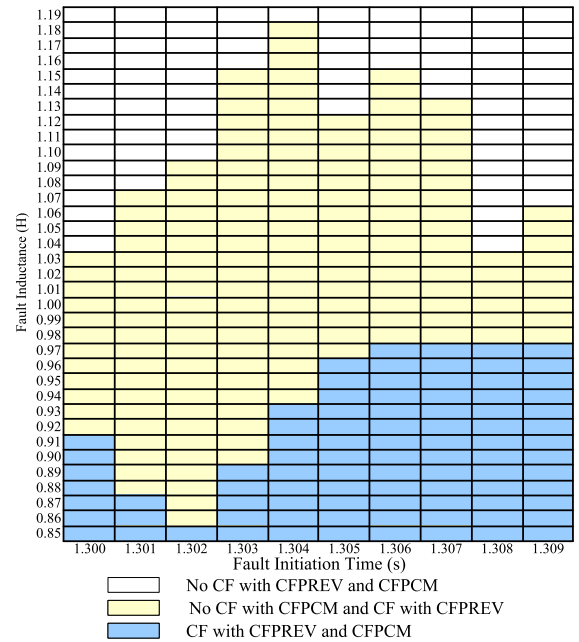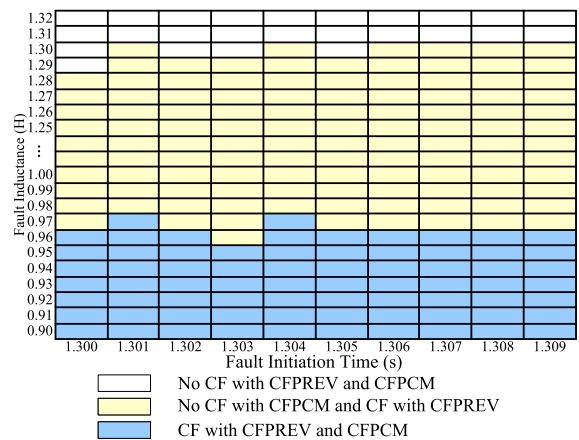
high value (Fig. 9(a1)). Compared to CFPREV, by applying CFPCM, the AC voltage decreases slowly and maintain a high value, and the DC current only changes slightly. In Fig. 9(b), when the L_f is 0.8 H, there is no CF in CFPREV and CFPCM. However, by applying CFPCM, the extinction angle, AC system, and DC current have a small fluctuation, because the CFPCM can control the firing angle accurately, and the reactive power consumed by inverter is smaller than that in CFPREV.

Similar to Fig. 9, as shown in Fig. 10 (a) and Fig. 11 (a), a CF occurred in the inverter by applying CFPREV, but no CF was observed by applying CFPCM. In Fig. 11(b), there is no CF with CFPREV and CFPCM, but the DC current and AC voltage changed smoothly. Fig. 11 shows the system
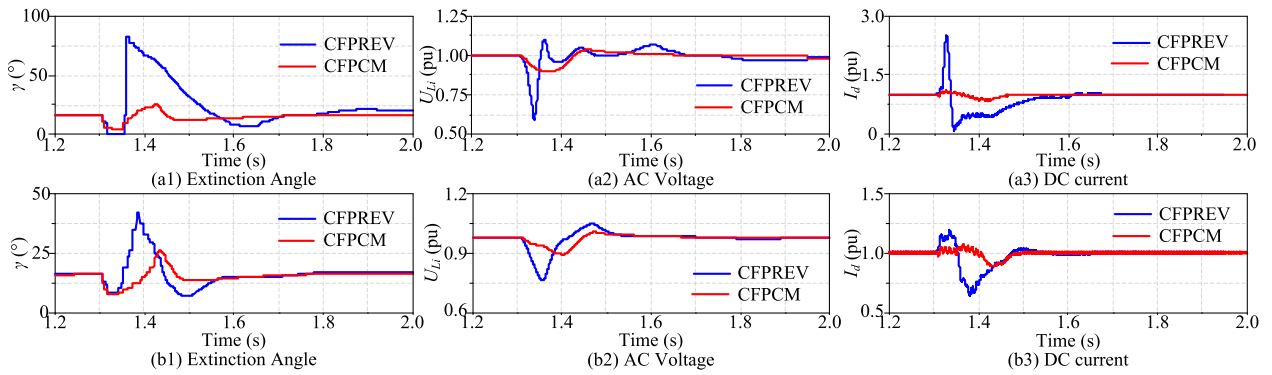
FIGURE 9. Simulation performance for the LG fault with CFPREV and CFPCM at 1.304 s. (a) L_f = 0.6 H and CFPREV faced CF only. (b) L_f = 0.8H and CFPREV and CFPCM all not faced commutation failure.
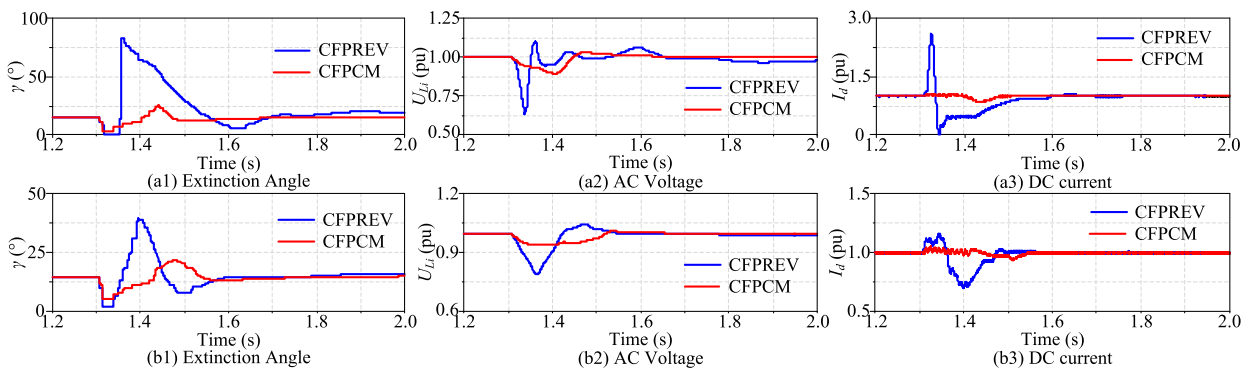
FIGURE 10. Simulation performance for the LLG fault with CFPREV and CFPCM at 1.304 s. (a) L_f =1 H and CFPREV faced CF only. (b) L_f =1.2 H and CFPREV and CFPCM all not faced commutation failure.
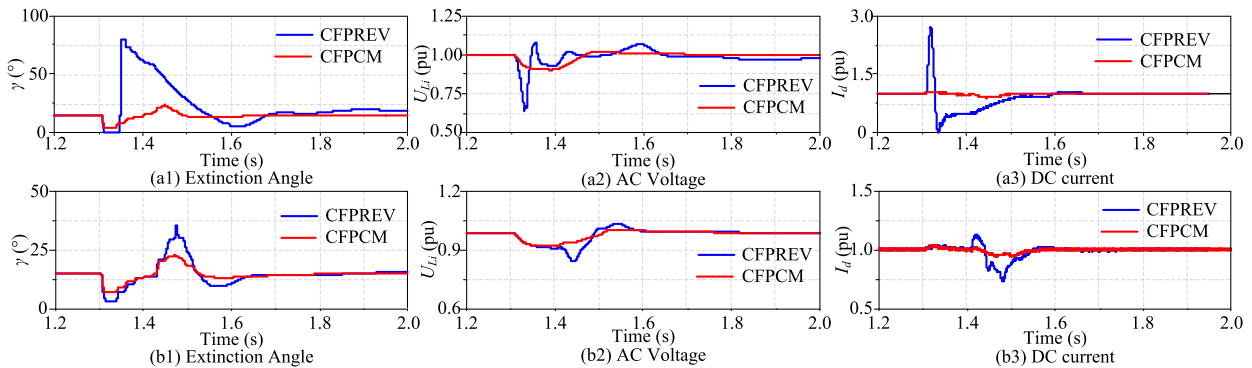
FIGURE 11. Simulation performance for the LLLG fault with CFPREV and CFPCM at 1.304 s. (a) L_f =1 H and CFPREV faced CF only. (b) L_f = 1.32 H and CFPREV and CFPCM all not faced commutation failure.

simulation results of γ, U_{Li}, and I_d under LLLG with L_f = 1 H and 1.32 H, respectively. In the case of L_f =1 H, there is only CFPREV facing CF, for L_f =1.32 H, the CFPREV and CFCCS are all not facing CF.

In summary, compared to CFPREV, the CFPCM proposed in this paper can inhibit CF more effectively. Moreover, in the case of no CF, the fluctuation in DC current, AC voltage, and extinction angle can be reduced by applying the CFPCM.

VI. DISCUSSION

As can be seen in (11), (12) and Fig. 5, the proposed method requires differentiation of voltage, the influence of voltage harmonic on the proposed method should be considered. Aiming at this problem, based on PSCAD/EMTDC simulation software and CIGRE HVDC system, take phase-a voltage as an example to perform Fast Fourier Transform (FFT). The Cases are set as follows:

Case 1: LG fault with L_f is 1 H at 1.3 s.
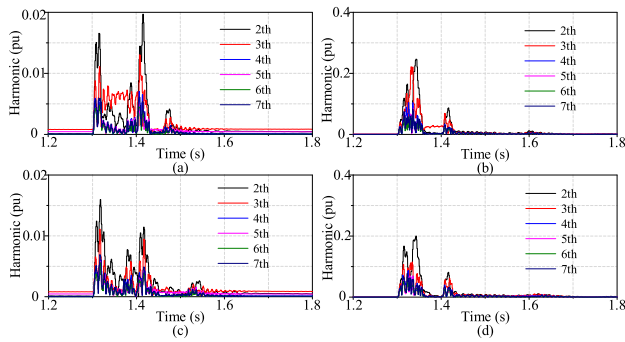
FIGURE 12. The FFT analysis results under different cases. (a) Case 1; (b) Case 2; (c) Case 3; (d) Case 4.
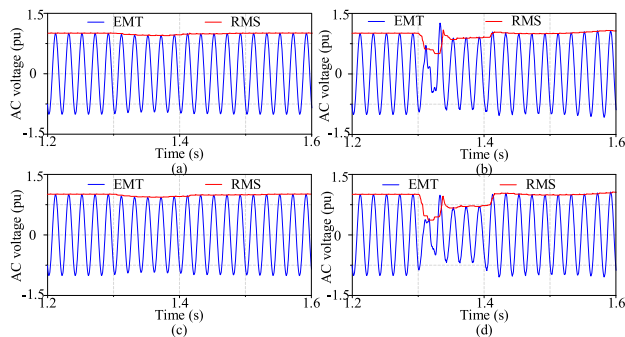
FIGURE 13. The RMS (the proposed method) and EMT voltage simulation results under different cases. (a) Case 1; (b) Case 2; (c) Case 3; (d) Case 4.

Case 2: LG fault with L_f is 0.2 H at 1.3 s.

Case 3: LLLG fault with L_f is 1.5 H at 1.3 s.

Case 4: LLLG fault with L_f is 0.2 H at 1.3 s.

In all the cases, the fault duration is 0.1 s. The FFT analysis results under different cases can be seen shown in Fig. 12.

In Fig. 12, For Case 1 and Case 3, there is no CF occurred, for Case 2 and Case 4, there is CF occurred.

As can be seen from Fig. 12, after an AC system fault, the interaction between AC and DC systems will lead to the increase of the voltage harmonic, which mainly contains the second harmonic and the third harmonic. When there is no CF (Case 1 and Case 3), the voltage harmonic is low, and the maximum harmonic amplitude is only 0.02 pu. However, when a CF occurred, the voltage harmonic increases sharply, and the maximum amplitude of the second harmonic reaches 0.25 pu. Therefore, before the CF, we believe that the harmonics will not have a great impact on the AC voltage amplitude detection method.

To further analyze the influence of harmonics on the proposed method after an AC system fault, the results of AC voltage (taking U_{ab} as an example) under different cases are shown in Fig.13.

It can be seen from Fig. 13 that when there is no CF occurred (Fig. 13 (a) and (c)), the RMS voltage results proposed in this paper are consistent with the EMT results. When a CF occurred (Fig.13 (b) and (d)), the proposed A method can characterize the voltage change trend. Although there is some error with the actual AC voltage instantaneous value during CF, considering the purpose of the proposed method
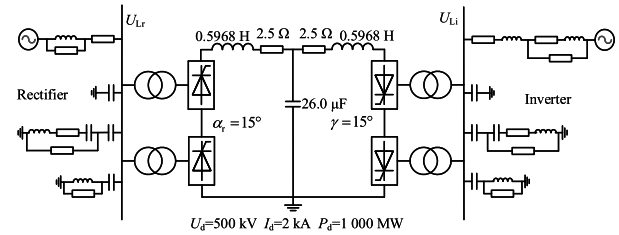
FIGURE 14. Simulation model structure.

in this paper is mainly to predict whether commutation failure will occur and decide whether to start CFPCM. Hence, before the CF, the proposed method can still accurately and quickly measure the AC voltage, which can predict whether the CF accurately.

VII. CONCLUSION

In this paper, the reason and mechanism of were analyzed for the different fault types. A fast AC voltage measurement method was proposed and proved to adapt to all fault types. Based on this method, a CF predictive control strategy was proposed. The simulation results in PSCAD under different fault types, fault inductances, and fault initiation times show that the CFPCM can inhibit CF more effectively. The CFPCM can also reduce the fluctuation of DC current, AC voltage, and exaction angle after LG, LLG, and LLLG fault. The proposed CFCCS can enrich the CF mechanism and provide a new idea to inhibit CF. In conclusion, only the theoretical analysis and simulation verification were carried out for single-HVDC, and the control strategy under the interaction of multi-HVDC needs further investigation. In the future work, the influence of harmonics on the proposed method will be further considered.

REFERENCES

[1] M. Li, "Characteristic analysis and operational control of large-scale hybrid UHV AC/DC power grids," *Power Syst. Technol.*, vol. 40, no. 4, pp. 985–991, 2016.

[2] X. Dong, Y. Tang, G. Bu, C. Shen, G. Song, Z. Wang, D. Gan, J. Hou, B. Wang, B. Zhao, and S. Shi, "Confronting problem and challenge of large scale AC-DC hybrid power grid operation," *Proc. Chin. Soc. Elect. Eng.*, vol. 39, no. 11, pp. 3107–3118, 2019.

[3] X. Dong, E. Guan, L. Jing, H. Wang, and S. Mirsaeidi, "Simulation and analysis of cascading faults in hybrid AC/DC power grids," *Int. J. Electr. Power Energy Syst.*, vol. 115, Feb. 2020, Art. no. 105492.

[4] Y. Li, "Technology and practice of the operation control of large power grid connected with weak AC area," *Power Syst. Technol.*, vol. 40, no. 12, pp. 3756–3760, 2016.

[5] C. Zheng, S. Ma, X. Shen, and D. Liu, "Definition, connotation and form of strong HVDC and weak AC and countermeasures for stable operation of hybrid power grid," *Power Syst. Technol.*, vol. 41, no. 8, pp. 2491–2498, 2017.

[6] Y. Zhu, S. Zhang, D. Liu, L. Zhu, S. Zou, S. Yu, and Y. Sun, "Prevention and mitigation of high-voltage direct current commutation failures: A review and future directions," *IET Gener., Transmiss. Distrib.*, vol. 13, no. 24, pp. 5449–5456, Dec. 2019.

[7] S. Ruan, K. Xu, D. Liu, P. Lyu, D. Wang, and H. Wang, "Statistical analysis and suggestions on resistance measures for commutation failures of HVDC transmission system," *Automat. Electr. Power Syst.*, vol. 43, no. 18, pp. 13–17, 2019.

[8] C. V. Thio, J. B. Davies, and K. L. Kent, "Commutation failures in HVDC transmission systems," *IEEE Trans. Power Del.*, vol. 11, no. 2, pp. 946–957, Apr. 1996.

[9] T. Machida and Y. Yoshida, "A method to detect the deionization margin angle and to prevent the commutation failure of an inverter for DC transmission," *IEEE Trans. Power App. Syst.*, vol. PAS-86, no. 3, pp. 259–262, Mar. 1967.

[10] F. Nishimura, A. Watanabe, N. Fujii, and F. Ogata, "Constant power factor control system for HVDC transmission," *IEEE Trans. Power App. Syst.*, vol. PAS-95, no. 6, pp. 1845–1853, Nov. 1976.

[11] A. Hansen and H. Havemann, "Decreasing the commutation failure frequency in HVDC transmission systems," *IEEE Trans. Power Del.*, vol. 15, no. 3, pp. 1022–1026, Jul. 2000.

[12] L. Zhang and L. Dofnas, "A novel method to mitigate commutation failures in HVDC systems," in *Proc. Int. Conf. Power Syst. Technol.*, 2002, pp. 51–56.

[13] J. Bauman and M. Kazerani, "Commutation failure reduction in HVDC systems using adaptive fuzzy logic controller," *IEEE Trans. Power Syst.*, vol. 22, no. 4, pp. 1995–2002, Nov. 2007.

[14] Y. Z. Sun, L. Peng, F. Ma, G. J. Li, and P. F. Lv, "Design a fuzzy controller to minimize the effect of HVDC commutation failure on power system," *IEEE Trans. Power Syst.*, vol. 23, no. 1, pp. 100–107, Feb. 2008.

[15] L. Liu, S. Lin, K. Liao, P. Sun, Y. Deng, X. Li, and Z. He, "Extinction angle predictive control strategy for commutation failure mitigation in HVDC systems considering voltage distortion," *IET Gener., Transmiss. Distribution*, vol. 13, no. 22, pp. 5171–5179, Nov. 2019.

[16] Q. Wang, C. Zhang, X. Wu, and Y. Tang, "Commutation failure prediction method considering commutation voltage distortion and DC current variation," *IEEE Access*, vol. 7, pp. 96531–96539, 2019.

[17] Z. Wei, Y. Yuan, X. Lei, H. Wang, G. Sun, and Y. Sun, "Direct-current predictive control strategy for inhibiting commutation failure in HVDC converter," *IEEE Trans. Power Syst.*, vol. 29, no. 5, pp. 2409–2417, Sep. 2014.

[18] Y. Yuan, Z. Wei, H. Wang, X. Lei, and G. Sun, "A DC current predictive control based method to decrease probability of commutation failure," *Power Syst. Technol.*, vol. 38, pp. 565–570, Mar. 2014.

[19] S. Mirsaeidi and X. Dong, "An enhanced strategy to inhibit commutation failure in line-commutated converters," *IEEE Trans. Ind. Electron.*, vol. 67, no. 1, pp. 340–349, Jan. 2020.

[20] S. Mirsaeidi, X. Dong, D. Tzelepis, D. M. Said, A. Dysko, and C. Booth, "A predictive control strategy for mitigation of commutation failure in LCC-based HVDC systems," *IEEE Trans. Power Electron.*, vol. 34, no. 1, pp. 160–172, Jan. 2019.

[21] Z. Wei, W. Fang, and J. Liu, "Variable extinction angle control strategy based on virtual resistance to mitigate commutation failures in HVDC system," *IEEE Access*, vol. 8, pp. 93692–93704, 2020.

[22] B. Zhou, F. Li, and C. Yin, "A novel method to predict and prevent commutation failures in LCC-HVDC systems," *Int. J. Electr. Power Energy Syst.*, vol. 144, Jan. 2023, Art. no. 108399.

[23] P. Wang, Y. Wang, N. Jiang, and W. Gu, "A comprehensive improved coordinated control strategy for a STATCOM integrated HVDC system with enhanced steady/transient state behaviors," *Int. J. Electr. Power Energy Syst.*, vol. 121, Oct. 2020, Art. no. 106091.

[24] X. Liu, Z. Cao, B. Gao, Z. Zhou, X. Wang, and F. Zhang, "Predictive commutation failure suppression strategy for high voltage direct current system considering harmonic components of commutation voltage," *Processes*, vol. 10, no. 10, p. 2073, Oct. 2022.

[25] C. Guo, C. Li, C. Zhao, X. Ni, K. Zha, and W. Xu, "An evolutional line-commutated converter integrated with thyristor-based full-bridge module to mitigate the commutation failure," *IEEE Trans. Power Electron.*, vol. 32, no. 2, pp. 967–976, Feb. 2017.

[26] Y. Xue, X. Zhang, and C. Yang, "Commutation failure elimination of LCC HVDC systems using thyristor-based controllable capacitors," *IEEE Trans. Power Del.*, vol. 33, no. 3, pp. 1448–1458, Jun. 2018.

[27] E. Rahimi, A. M. Gole, J. B. Davies, I. T. Fernando, and K. L. Kent, "Commutation failure analysis in multi-infeed HVDC systems," *IEEE Trans. Power Del.*, vol. 26, no. 1, pp. 378–384, Jan. 2011.

[28] M. O. Faruque, Y. Zhang, and V. Dinavahi, "Detailed modeling of CIGRÉ HVDC benchmark system using PSCAD/EMTDC and PSB/SIMULINK," *IEEE Trans. Power Del.*, vol. 21, no. 1, pp. 378–387, Jan. 2006.

[29] C. Yin and F. Li, "A novel evaluation method for the risk of simultaneous commutation failure in multi-infeed HVDC-systems that considers DC current rise," *Int. J. Electr. Power Energy Syst.*, vol. 131, Oct. 2021, Art. no. 107051.

GUODONG HUANG was born in January 1977. He received the bachelor's degree in electrical engineering from North China Electric Power University, in June 1998. He is currently a deputy senior engineer. His research interests include the power distribution Internet of Things, power distribution automation, and smart power distribution networks.

XIAO TIAN was born in June 1999. He is currently pursuing the master's degree with the Faculty of Electric Power Engineering, Kunming University of Science and Technology. His research interests include power distribution Internet of Things, power distribution automation, and smart power distribution networks.

HAIBO YUAN, photograph and biography not available at the time of publication.

XIAOFENG DONG was born in August 1984. He received the master's degree in electrical engineering from Southeast University, in March 2010, and the Ph.D. degree in electrical engineering from North China Electric Power University, in August 2020. He is currently a deputy senior engineer. His research interests include the power distribution Internet of Things, power distribution automation, and smart power distribution networks.

LI ZHOU was born in August 1992. He received the master's degree in electrical engineering from Southeast University, in June 2017. He is currently a deputy senior engineer. His research interests include power distribution automation, feeder automation, and smart power distribution networks.

QING WANG was born in June 1989. He received the Ph.D. degree in electrical engineering from North China Electric Power University, in June 2016. He is currently a deputy senior engineer. His research interests include the power distribution Internet of Things, power distribution automation, and smart power distribution networks.

• • •